DYNAMIC ANALYSIS OF TOOL CHANGING SYSTEM IN POWER TOOL TOWER

Qianqian WANG [1,*], Song LIANG [2]

Dynamic characteristic is important for the tool changing process of the numerically controlled machine. High efficiency and low energy waste can increase the output product per unit of time and thus have great significance to save production cost in the automobile, consumer electronics manufacturing and other high-productivity light industries. A two degrees of freedom system is utilized to simplify the dynamic model of tool changing system, and the dynamic parameters of each unit are calculated. Then the responses and the residual vibration of tool changing system at target position under T-type and S-type control curves are analyzed and compared.

Keywords: tool changing, dynamic, residual vibration, control curve

1. Introduction

Power tool tower is the most common automatic tool changing device in numerically controlled (NC) lathe and turning mill compound machining center. The execution efficiency of tool changing mechanism is an important design index of power tool tower. In high-productivity and low-margin industries such as the manufacturing of motor vehicles and consumer electronics, output per unit of time has a significant impact on production costs. The individual products in these industries are less profitable, but the number of products is large and the overall profits of the industry are considerable. With this scale effect in productivity industries, even a tenth of a second of manufacturing time saved on a production line can yield significant economic benefits. The tool changing time of power tool tower module in NC machine tool belongs to auxiliary processing time and is not directly used in workpiece manufacturing. In the manufacture of parts that require more than one tool fit, shorter changeover times mean higher productivity.

The dynamic analysis of tool changing system in power tool tower belongs to the research field of high speed precise indexing mechanism. Many scholars have made positive contributions to it. For example, Jiang et al. [1,2] studied vibration suppression of high - speed indexing mechanism by using B-spline method with dynamic compensation, and proposed an optimal method for

[1] PhD, School of Mechanical electronic and Vehicle Engineering, WeiFang University, China
[2] PhD, School of Mechanical Engineering , Shenyang University of Technology, China
* Corresponding author: Qianqian WANG, email: neu_wqq@163.com

vibration suppression of high speed indexing mechanism. Lian et al. [3] proposed a novel method to design high-speed cam profiles for vibration reduction by using command smoothing technique. Renn et al. [4] took a hydraulic cam-style lathe tool tower as a research object using the method of load induction control to reduce the energy loss in the process of tool change. Tsay et al. [5-8] studied mathematical description method of cams surface, and then the dynamic model of cam indexing drive system is established for the purpose of designing the torque balance system of cam indexing mechanism. In view of the residual vibration problem of cam indexing system, Sateesh et al. [9] and Qiu al. [10] proposed an optimal design method of cam indexing system. These references are mainly focused on the cam indexing system as well as references [11,12]. However, as the development of servo control technology is becoming mature, the combination of alternating current servo motor and multi-stage gear drive has become the mainstream configuration of middle and high grade power servo tower system [13,14]. So it is necessary to pay more attention on the gear transmission system. As gear dynamic analysis is widely researched in references [15-17], it provides methods for solving similar problems.

The main work of this paper is to study the tool changing system of a type of power servo tool tower. A two-degree-of-freedom dynamic model of wheel-type tool change system is established. Based on the dynamic model of tool changing system, the response characteristics of control curves of T and S type motion are analyzed respectively. The dynamic response of the cutter head during the tool changing process and the residual vibration of the tool changing system at the target position are discussed.

2. Dynamic Model of the System

2.1. Dynamics of Tool Changing Process

The transmission schematic diagram of the tool changing mechanism of a kind of power servo tool tower is shown in Fig. 1, which is composed by the dynamic system components, speed reduction components and cutter components. The components of the dynamic system contain a servo motor and its controller system, which decides the motion curve of the motor.

J_0 denotes the inertia of moment of the motor, while J_1, J_{23}, J_{45}, J_6 represent the inertia of moment of each transmitting shaft in the three-stage gear reduction system respectively. As the gear reduction system is complex in dynamic analysis, an equi-power principle is implemented to simplify the reduction system to a single degree of freedom concentrated mass system, in which J_M, K_M and C_M are the equivalent inertia of moment, equivalent torsional stiffness coefficient and equivalent torsional damping coefficient respectively.

The load of the system is composed by the spindle, cutter and several driven tool, with the inertia of moments denoted as J_s, J_{disc} and J_{tool} respectively.

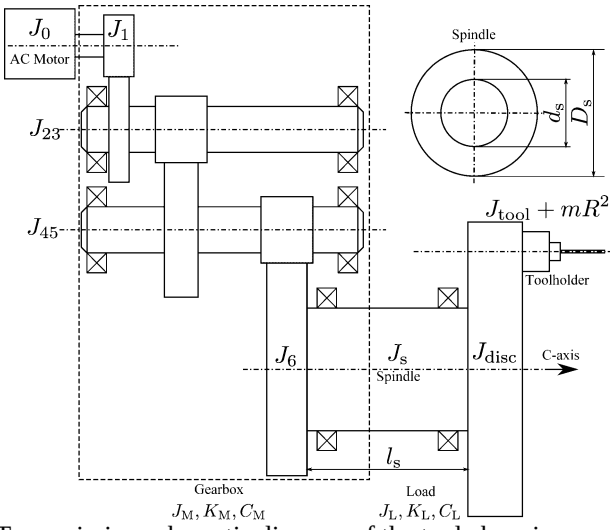

Fig. 1. Transmission schematic diagram of the tool changing mechanism

Fig. 2 is the simplified dynamic model of the tool changing mechanism, which is a two-degree-freedom concentrated mass system.

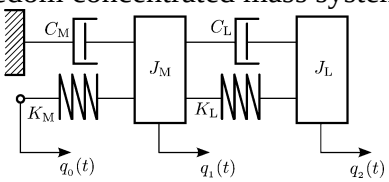

Fig. 2. Simplified dynamic model of the tool changing mechanism

The dynamic differential equations can be obtained by the Newton's law:

$$\boldsymbol{M}\ddot{\boldsymbol{q}} + \boldsymbol{C}\dot{\boldsymbol{q}} + \boldsymbol{K}\boldsymbol{q} = \boldsymbol{Q}(t) \tag{1}$$

where $q = (q_1, q_2)^{\mathrm{T}}$, $\boldsymbol{Q}(t) = (K_M q_0(t), 0)^{\mathrm{T}}$.

According to the non-damping free vibration differential equation, the first natural frequency of the system can be obtained as:

$$\omega_{n1}^2 = \frac{-b - \sqrt{b^2 - 4ac}}{2a} \tag{2}$$

in which $a = J_M J_L$, $b = -\left[-K_L J_M + (K_M + K_L) J_L\right]$, $c = -K_L (K_M + K_L) - \left(-K_L\right)^2$.

2.2. Motion Control Curve of System and Residual Vibration Coefficient

Fig. 3 gives the displacement curve, velocity curve and acceleration curve of the T type motion control curve.

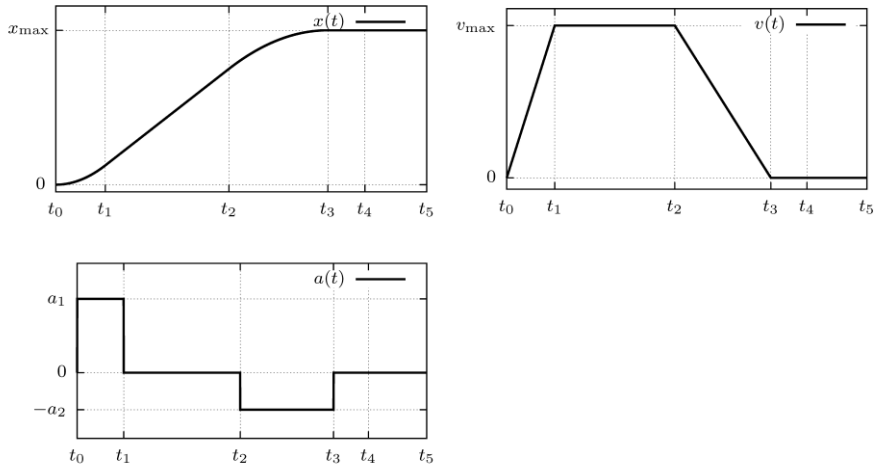

Fig. 3. Characteristic curves of T-type control curve

Fig. 4 gives the displacement curve, velocity curve, acceleration curve and jerk diagram of the S type motion control curve.

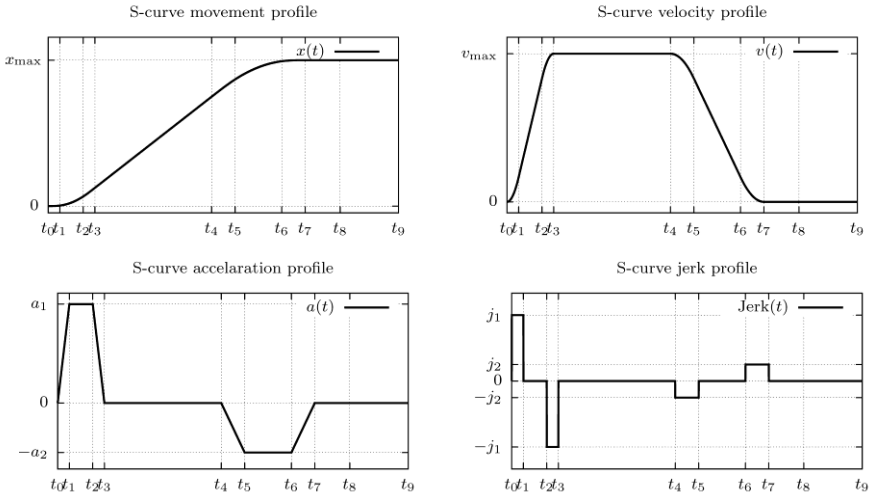

Fig. 4. Characteristic curves of T-type control curve

T-type and S-type motion control curves are the common motion curves of high-speed indexing mechanism. The control algorithm of T-type curve is simple and has low requirement on hardware performance. Although the control algorithm of S-type curve is complex, which requires high hardware performance, it has no flexible impact and small residual vibration.

The formula calculating residual vibration coefficient at a supposed point *A* is:

$$M_A = \sqrt{(X_A - 1.0)^2 + \left(\frac{V_A}{\omega_n}\right)^2} \tag{3}$$

where ω_n is the first natural frequency of the system, which can be calculated by Eq.(2). X_A and V_A are the dimensionless motion parameters. The subscript A of all the parameters means the value at point A is used in the calculation program.

Another result parameter called characteristic value of dynamic load torque is introduced to analysis the performance of the tool changing system which is defined as:

$$(AV)_m = \max(A \cdot V) - \min(A \cdot V) \tag{4}$$

where $A \cdot V$ means the product of dimensionless acceleration and velocity of the dynamic cutter during the tool change cycle, the value of which is proportional to the instantaneous torque of the spindle of the cutter tower. The energy efficiency of the system in the process of tool change can be measured by $(AV)_m$, and smaller value means higher energy efficiency of the system.

3. Calculation of Dynamic Parameters of the System

3.1. Calculation of Moment of Inertia in Gear Transmission System

The formula for calculating the moment of inertia of gear tooth is:

$$J_{\text{teeth}} = zB\rho \int_{r_f}^{r_a} r_k^2 s(r_k)\, \mathrm{d}r_k = zB\rho(I_1 + I_2) \tag{5}$$

where B is the tooth width; ρ is the density of the material; z is the number of teeth; r_k is the distance of an arbitrary point on the tooth surface to the gear center; and $s(r_k)$ is the circular thickness of the arbitrary point, with the interval $r_k \in [r_f, r_a]$.

The cross section moment of inertia of the transition curve of the tooth root I_1 and the moment of inertia of the involute part I_2 are given as:

$$I_1 = \int_{r_f}^{r_M} r_k^2 s(r_k)\, \mathrm{d}r_k, \quad I_2 = \int_{r_M}^{r_a} r_k^2 s(r_k)\, \mathrm{d}r_k. \tag{6}$$

where M is the intersection point of the transition curve between the involute tooth surface and the tooth root.

The moment of inertia of the gear is:

$$J = J_{\text{Body}} + J_{\text{teeth}} \tag{7}$$

According to the simplified model of Gear1, Gear23, Gear45 and Gear6 in Fig. 5, the moment of inertia of each shaft can be expressed as:

$$\begin{cases} J_1 = J_{\text{teeth1}} + \dfrac{1}{32}\rho[(l_1 - B_1)D_1^4 + B_1 D_{f_1}^4 - l_1 d_1^4] \\ J_{23} = J_{\text{teeth2}} + J_{\text{teeth3}} + \dfrac{1}{32}\rho[(l_{23} - B_2 - B_3)D_{23}^4 + B_2 D_{f_2}^4 + B_3 D_{f_3}^4] \\ J_{45} = J_{\text{teeth4}} + J_{\text{teeth5}} + \dfrac{1}{32}\rho[(l_{45} - B_4 - B_5)D_{45}^4 + B_4 D_{f_4}^4 + B_5 D_{f_5}^4] \\ J_6 = J_{\text{teeth6}} + \dfrac{1}{32}\rho[(l_6 - B_6)D_6^4 + B_6 D_{f_6}^4 - l_6 d_6^4] \end{cases} \tag{8}$$

The equivalent moment of inertia of the gear drive system with respect to the *C* axis can be obtained:

$$J_M = (J_0 + J_1)\left(\frac{\omega_1}{\omega_6}\right)^2 + J_{23}\left(\frac{\omega_{23}}{\omega_6}\right)^2 + J_{45}\left(\frac{\omega_{45}}{\omega_6}\right)^2 + J_6 \tag{9}$$

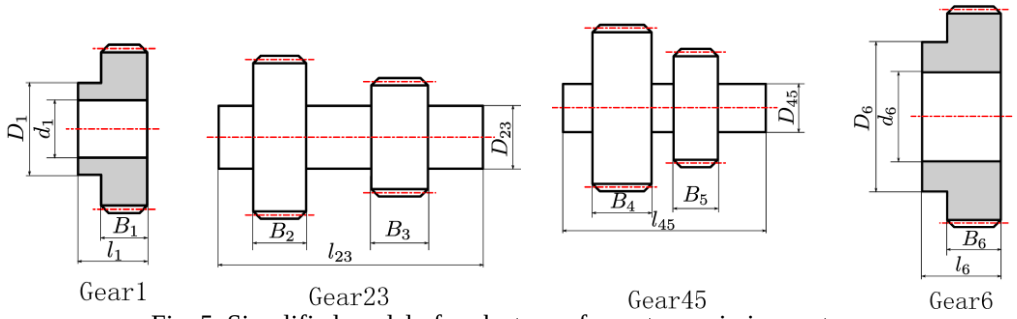

Fig. 5. Simplified model of each stage of gear transmission system

3.2. Calculation of Equivalent Torsional Stiffness and Damping Coefficient of Gear Transmission System

According to Weber method [15], synthesized meshing stiffness of each gear pair is calculated. Therefore, the meshing stiffness of the gear transmission considering tooth width is expressed as:

$$k_{m12} = \min\{B_1, B_2\} \times \bar{k}_{1,2},\ k_{m34} = \min\{B_3, B_4\} \times \bar{k}_{3,4},\ k_{m56} = \min\{B_5, B_6\} \times \bar{k}_{5,6} \tag{10}$$

where $\bar{k}_{1,2}$, $\bar{k}_{3,4}$, $\bar{k}_{5,6}$ are the average synthesized meshing stiffness of each gear pair.

Ignoring the torsional stiffness of the gear shaft, the equivalent torsional stiffness of the gear system is obtained:

$$\frac{1}{K_M} = \frac{1}{r_{b1} r_{b2} k_{m12}}\left(\frac{\omega_{23}}{\omega_1}\right)^2 + \frac{1}{r_{b3} r_{b4} k_{m34}}\left(\frac{\omega_{45}}{\omega_1}\right)^2 + \frac{1}{r_{b5} r_{b6} k_{m34}}\left(\frac{\omega_6}{\omega_1}\right)^2$$

in which $r_{bi}(i = 1, 2, \cdots, 6)$ is the radius of the basic circle.

The viscous damping is expressed as:

$$C_{m12}=2\xi_m\sqrt{\frac{k_{m12}}{\frac{r_{b1}^2}{J_0+J_1}+\frac{r_{b2}^2}{J_{23}}}},\ C_{m34}=2\xi_m\sqrt{\frac{k_{m34}}{\frac{r_{b3}^2}{J_{23}}+\frac{r_{b4}^2}{J_{45}}}},\ C_{m56}=2\xi_m\sqrt{\frac{k_{m56}}{\frac{r_{b5}^2}{J_{45}}+\frac{r_{b6}^2}{J_6}}} \tag{11}$$

in which $\xi_m=0.1$, and the comprehensive damping coefficient C_m can be decided by the moment of inertia and the meshing stiffness of the system. Therefore, the equivalent torsional damping coefficient of the gear transmission system is obtained:

$$C_M=C_{m12}r_{b1}r_{b2}\left(\frac{\omega_1}{\omega_6}\right)^2+C_{m34}r_{b3}r_{b4}\left(\frac{\omega_{23}}{\omega_6}\right)^2+C_{m56}r_{b5}r_{b6}\left(\frac{\omega_{45}}{\omega_6}\right)^2 \tag{12}$$

4. Results

The parameters of the gear transmission system are shown in Table 1. In this section, the Newmark method is implemented to solve the dynamic differential equation.

Table 1

List of design parameters in the gear system

Gear Number	Modulus [mm]	Number of Teeth	Modification Coefficient	Tooth Width [mm]
Gear1	1.5	18	0.4	18.0
Gear2	1.5	54	-0.4	14.0
Gear3	1.75	13	0.3	20.0
Gear4	1.75	52	-0.3	15.0
Gear5	3.00	9	0.33	31.0
Gear6	3.00	54	0.00	26.5

The dynamic parameters in the tool changing system can be calculated using the method in section 3. The results of the dynamic parameters are:
J_M =1.3584Kg·m^2, K_M= 1.7599×10^{6}N·m·rad^{-1}, C_M=6.60659×10^3 N·m·s·rad^{-1},
J_L= 7.8855 Kg·m^2, K_L=5.6828×10^{6}N·m·rad^{-1}, C_L= 6.0042×10^3 N·m·s·rad^{-1}.

4.1. Dynamic Analysis of the T Type Control Curve System

In this section, the dynamic response of the tool change system under the excitation of T-type motion control curve is calculated. Table 2 gives the design parameters of the T-type control curve.

Table 2

Design parameters of T-type motion program

Parameter	Symbol	Unit	Value
Maximum speed of cutter head	v_{max}	deg/s	187.5
Acceleration time	T_1	s	0.040
Braking time	T_2	s	0.080

The result curves are in Fig. 6, containing displacement curves, velocity curves and acceleration curves of the input $q_0(t)$ and output $q_2(t)$.

Fig. 7 shows the residual vibration curves of the system which are the velocity and acceleration curves extracted from Fig. 10 in the time interval [0.200, 0.300]. When t=0.220, the input curve reached its target location while the output curve didn't reach the target location. That is why the residual vibration exists.

Fig. 8 shows the curves of dynamic load torque characteristic value of the tool changing system under T-type excitation. As it is shown, two peaks appear near the transition point of the acceleration segment and the constant velocity segment, the transition point of the constant speed segment and the deceleration segment respectively. Meanwhile, the output torque of the servo motor also reaches its peaks, which means torque jump exists.

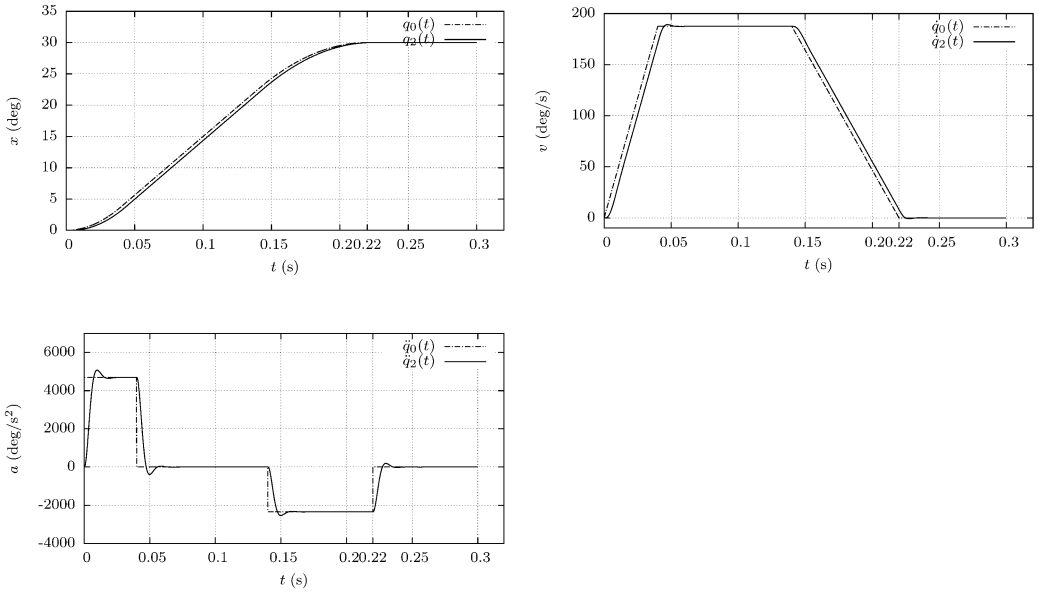

Fig. 6. T-type dynamics response curve of the tool changing system

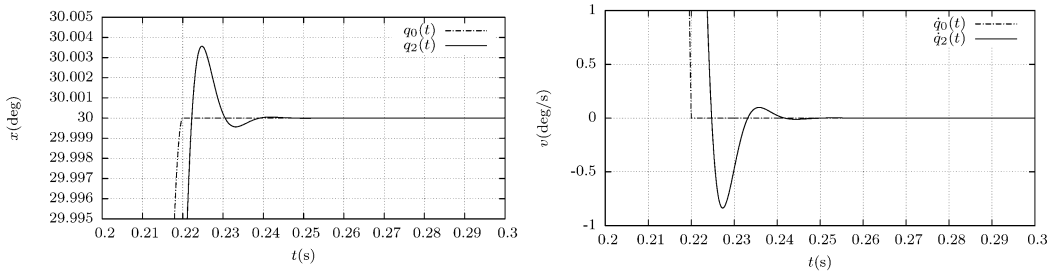

Fig. 7. Residual vibration of T-type tool changing system

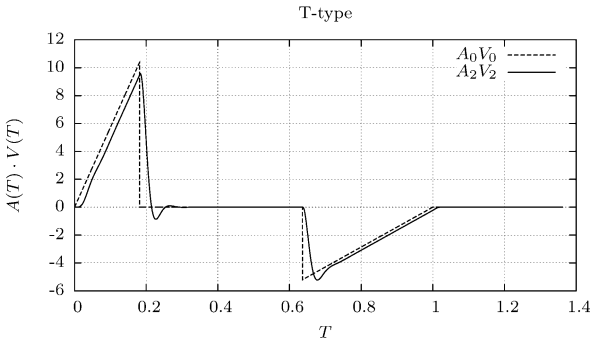

Fig. 8. T-type dynamic load torsion eigenvalue curve of the tool changing system

The residual vibration coefficient M_A=4.23×10^{-4} is calculated at t=0.220, when the input reached the target location.

The analysis of the dynamic response curve shows that the actual output displacement and velocity of the power cutter are always different from the input displacement and velocity of the servo motor because of the existence of elastic deformation. When the servo motor input displacement q_0 reaches the target position (t=0.220s), the displacement and velocity of the power cutter are not zero.

Within the time interval $t \in [0.220, 0.300]$, the system is in a damped oscillation state, and the vibration energy of the power cutter gradually decreases and finally converges to zero.

4.2. Dynamic Analysis of the S Type Control Curve System

Similar to the T-type excitation, the S-type motion control curve is also the displacement excitation of the servo motor to the tool change system. The dynamic responses of the tool change system under the excitation of S-type motion control curve are calculated in this section.

Table 3 gives the design parameters of the S-type control curve.

Table 3

Design parameters of S-type motion program

Parameter	Symbol	Unit	Value
Maximum speed of cutter head	v_{max}	deg/s	187.5
Acceleration time	T_1	s	0.040
Braking time	T_2	s	0.080
starting acceleration	a_1	deg/s^2	9.375×10^3
braking acceleration	a_2	deg/s^2	4.688×10^3

The response curves are shown in Fig. 9, which contains the input and output curves of displacement, velocity and acceleration. Compared with the response curves of T-type control curve, the output curves perform higher similarity with the input curves in S-type excitation system, and the system can brake more smoothly.

Fig. 10 shows the residual vibration curves of the system which are the velocity and acceleration curves extracted from Fig. 9 in the time interval [0.200, 0.300]. Comparing with Fig. 7, the maximum overshoot of the S-type system is smaller, with shorter residual vibration time.

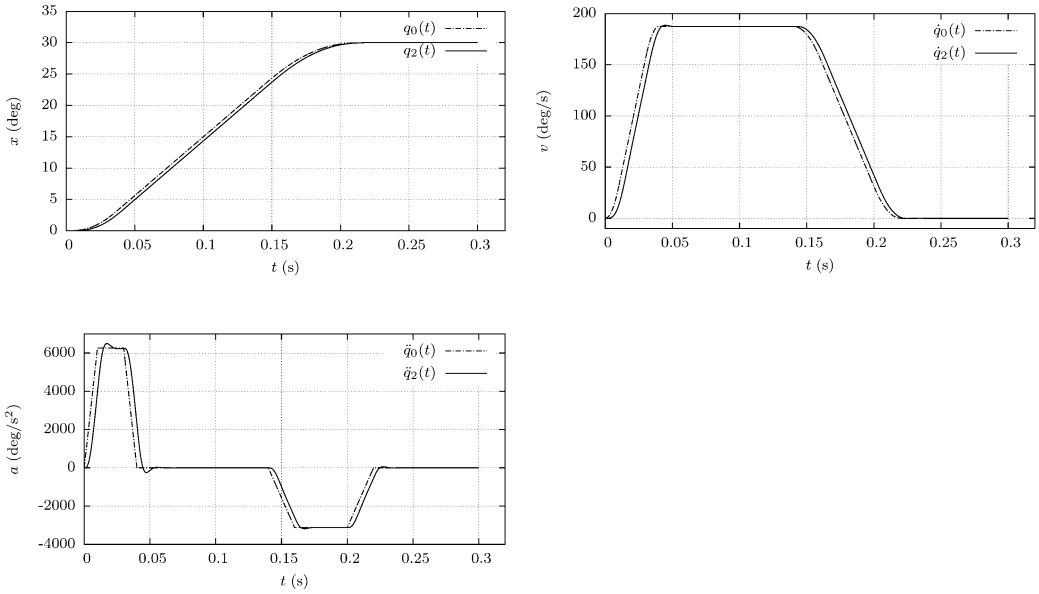

Fig. 9. S-type dynamic response curve of the tool changing system

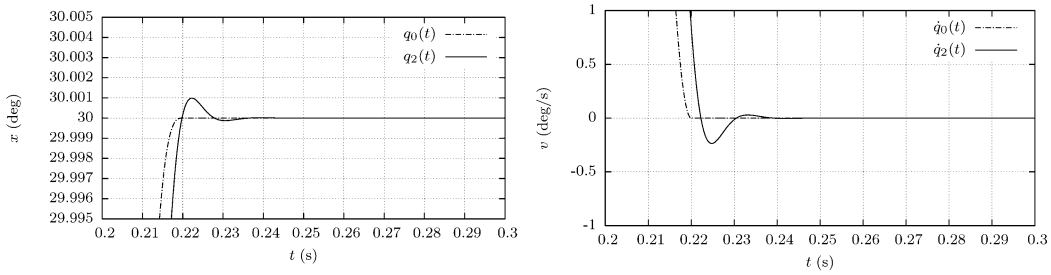

Fig. 10. Residual vibration of S-type tool changing system

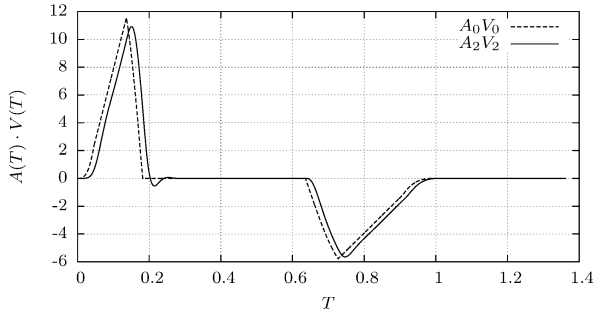

Fig. 11. S-type dynamic load torsion eigenvalue curve of the tool changing system

The curves of dynamic load torque characteristic value of the tool changing system under S-type excitation are shown in Fig. 11. Comparing with Fig. 8, the characteristic values of dynamic load torque of S-type system vary more widely, and the system energy consumption is higher.

5. Discussion and Conclusion

The method proposed in the paper studied a simplified transmission system by the equi-power method, which saves the calculation process and avoids complex calculation process for the multi-degree-of-freedom gear system as in the reference [18,19]. Although many indexing systems are composed by cam indexing mechanism, the profile of the cam contributes much on the system vibration and residual vibration. Optimization of the cam profile can reduce the vibration which is researched by Jiang et al. [1] and Xia et al. [20]. Comparing with the vibration results, the gear transmission system is smooth, with less response lag and easy to design.

The T-type and S-type design schemes are compared from the perspective of dynamic response analysis of the tool changing system. The residual vibration coefficient and the maximum overshoot of the S-type system are significantly lower than those of the T-type system. But the variation range of dynamic load torque characteristic value $(AV)_m$ of S-type system is significantly higher than that of T-type system. This fully shows that the S-type motion control method can significantly reduce the residual vibration level of the tool change system, making the cutter changing process fast and stable, which also increases the whole machine energy consumption of the system. Obviously, it must be noticed that the design idea of S-type scheme is to sacrifice energy utilization efficiency for motion stability. It is worth noting that the complexity of the control algorithm of the S-type scheme is higher than that of the T-type scheme, which has higher requirements on the control system.

REFERENCES

[1] *J. K. Jiang, Y. R. Iwai*, "Improving the B-Spline Method of Dynamically-Compensated Cam Design by Minimizing or Restricting Vibrations in High-Speed Cam-Follower Systems", in Journal of Mechanical Design, **vol. 131**, no. 4, 2009, pp. 041003, 1-8.

[2] *J. K. Jiang, Y. R. Iwai, H. Su*, "Minimizing and restricting vibrations in high-speed cam-follower systems over a range of speeds", in Journal of Applied Mechanics-Transactions of the ASME, **vol. 74**, no. 6, 2007, pp. 1157-1164.

[3] *Z. Liang, J. Huang*, "Design of high-speed cam profiles for vibration reduction using command smoothing technique", in Proceedings of the Institution of Mechanical Engineers, Part C: Journal of Mechanical Engineering Science, **vol.** 228, no. 18, 2014, pp. 3322-3328.

[4] *J. C. Renn, W. J. Hsu, W. C. Liao*, "Energy efficient lathe turret design using load sensing control scheme", in Proceedings 2014 International Symposium on Computer, Consumer and Control, IS3C 2014. Taichung, Taiwan: 2014, pp. 51-54.

[5] *D. M. Tsay, B. J. Lin*, "Design and Machining of Globoidal Index Cams", in Journal of Manufacturing Science and Engineering, **vol. 119**, no.1, 1997, pp. 21-29.
[6] *D. Tsay, H. Chen, S. Lin*, "A direct method for determining meshing surfaces of globoidal cams with tapered roller followers", in Proceedings of the Institution of Mechanical Engineers, Part C: Journal of Mechanical Engineering Science, **vol. 223**, no. 7, 2009, pp. 1667-1676.
[7] *D. M. Tsay, C. H. Liu, S. Y. Ho*, "Vibrational analysis and experimental implementation of rotational indexing mechanisms", in Proceedings of IMECE03, 2003 ASME International Mechanical Engineering Congress. Washington, DC, USA, 2003, p. 41630.
[8] *D. M. Tsay, H. C. Ho, K. C. Wang*, "Design of Torque Balancing Cams for Globoidal Cam Indexing Mechanisms", in Journal of Mechanical Design, **vol. 124**, no. 3, 2002, pp. 441-447.
[9] *N. Sateesh, C. S. P. Rao*, T. A. Janardhan Reddy, "Optimization of cam-follower motion using B-splines", in International Journal of Computer Integrated Manufacturing, **vol. 22**, no. 6, 2009, pp. 515-523.
[10] *H. Qiu, C. J. Lin, Z. Y. Li*, et al., "An Optimal Approach of Cam Curves to Control the Residual Vibration with Indexing Cam Mechanism", in Transactions of the Japan Society of Mechanical Engineers Series C, **vol. 69**, no. 682, 2003, pp. 1684-1690.
[11] *Y. H. Yang*, et al., "Design of a novel coaxial eccentric indexing cam mechanism", in Mechanism and Machine Theory, **vol. 132**, 2019, pp.1-12.
[12] *M. T. Liu*, et al., "Theoretical and experimental research on dynamics of the inner displaced indexing cam mechanism", in Mechanism and Machine Theory, **vol. 105**, 2016, pp. 620-632.
[13] *F. Y. Zheng*, et al., "Synthesis of indexing mechanisms with non-circular gears", in Mechanism and Machine Theory, **vol. 105**, 2016, pp. 108-128.
[14] *N. V. Zakharenkov, I. N. Kvasov*, "The kinematics and strength study of indexing bevel gear mechanism in rotating device driver", in Journal of Physics: Conference Series. IOP Publishing, 2018. pp. 012100.
[15] *Q. Wang, B. Zhao, X. Kong, H. Ma, J. Chang*, "Time-varying mesh stiffness analysis of a single-roller enveloping hourglass worm gear", in Proceedings of the Institution of Mechanical Engineers, Part C: Journal of Mechanical Engineering Science, **vol. 233**, no. 2, 2019, pp. 578-592.
[16] *Q. Wang, B. Zhao, Y. Fu, X. Kong, H. Ma*, "An improved time-varying mesh stiffness model for helical gear pairs considering axial mesh force component", in Mechanical Systems and Signal Processing, **vol. 106**, 2018, pp. 413-429.
[17] *D. Stoica, et al*., "Analysis of vibrations of conical sieves with oscillating motion using labview", in Scientific Bulletin, Series D, **vol. 82**, no. 1, 2020, pp. 43-54.
[18] *M. Dumitriu, and I. C. Cruceanu*, "Effect of vertical track irregularities on the vibration of railway bogie", in Scientific Bulletin, Series D, **vol. 81**, no. 1, 2019, pp. 67-77.
[19] *J. G. Wang, et al*., "Nonlinear characteristics of a multi-degree-of-freedom spur gear system with bending-torsional coupling vibration", in Mechanical Systems and Signal Processing, **vol. 121**, 2019, pp. 810-827.
[20] *B. Z. Xia, et al*., "Improving cam profile design optimization based on classical splines and dynamic model", in Journal of Central South University, **vol. 24**, no. 8, 2017, pp. 1817-1825.